

International Journal of Modern Physics E  
 © World Scientific Publishing Company

## The attribute of rotational profile to the hyperon puzzle in the prediction of heaviest compact star

M. Bhuyan<sup>1,2\*</sup>, B. V. Carlson<sup>2</sup>, S. K. Patra<sup>3</sup>, Shan-Gui Zhou<sup>1,4,5</sup>

<sup>1</sup>*Key Laboratory of Theoretical Physics, Institute of Theoretical Physics, Chinese Academy of Sciences, Beijing 100190, China*

<sup>2</sup>*Instituto Tecnológico de Aeronáutica, 12.228-900 São José dos Campos, São Paulo, Brazil*

<sup>3</sup>*Institute of Physics, Sachivalaya Marg, Sainik School, Bhubaneswar 751005, India*

<sup>4</sup>*Center of Theoretical Nuclear Physics, National Laboratory of Heavy Ion Accelerator, Lanzhou 730000, China*

<sup>5</sup>*Synergetic Innovation Center for Quantum Effects and Application, Hunan Normal University, Changsha, 410081, China*

In this theoretical study, we report an investigation of the equations of state (EoSs) of hyper-nuclear matter and its composition as a function of density within the framework of effective field theory motivated relativistic mean field model. We have used G2 force parameter along with various hyperon-meson coupling ratios by allowing the mixing and the breaking of SU(6) symmetry to predict the EoSs, keeping the nucleonic coupling constant intact. We have estimated the properties of non-rotating and rapidly rotating configuration of compact stars by employing four different representative sets of equations of state. The obtained results of the mass and radius for the compact stars are compared with the recent mass observations. Further, we have studied the stability and sensitivity of rotational frequency (at sub-millisecond period) on the configuration of the compact stars, because the angular frequency is significantly smaller than the mass-shedding (Keplerian) frequency in slow rotation regime. Moreover, the yield of hyperon as a function of density for various hyperon-meson couplings are also estimated.

*Keywords:* Relativistic mean field theory; Nuclear matter; Neutron star matter; Rotating neutron star

### 1. Introduction

The first theoretical idea of neutron stars comes from Baade and Zwicky,<sup>1</sup> being based on the analysis of supernova explosions. According to them, supernova explosion could be a transition from a star to a neutron star, consisting of closely packed neutrons in a compact size object. After a few years, the derivation of the full general relativistic equation of hydrostatic equilibrium for spherically symmetric objects, now known as *Tolman-Oppenheimer-Volkoff* (TOV) equation<sup>2</sup> came into figure. These equations were solved by Oppenheimer and Volkoff<sup>3</sup> assuming that the matter consisted of non-interacting neutrons, and found that the maximal allowed

\*Email:bunuphy@yahoo.com

mass for this to be  $0.71M_{\odot}$ . Later it was noticed that the inclusion of nuclear energy from the interacting neutrons increases this value substantially.<sup>4</sup> Observational proof for the existence of neutron star was obtained by Jocelyn Bell and Antony Hewish in 1967 by observing the pulsating radio beams from objects named pulsars, the rotating neutron stars with a strong magnetic field.<sup>4-6</sup> Generally, the behavior of matter in the interior of a neutron star is governed by the internal pressure, where all the neutrons obey the  $\beta$ -equilibrium condition with leptons and protons. An extended review of theoretical and observational aspects of neutron star, from the surface to the core, with the emphasis on their structure and equations of state can be found in Ref.<sup>6</sup> Further it is well known that the integral parameter for a foolproof structure of neutron star depends on their equation of state from an ideal theory, which can explain the  $\beta$ -equilibrium condition at high density. At present, a wide spectrum of different EoS for neutron star matters has been designed from different interactions such as Skyrme,<sup>7</sup> the Akmal-Pandharipande-Ravenhall<sup>8</sup> and the relativistic mean field theory (RMF)<sup>9</sup> (see Refs.<sup>6,10,11</sup> for reviews and the references therein for details). An extensive investigation on the EoS from these models show that they have almost similar properties at the nuclear saturation density (matter where the density of protons is equal to that of the neutrons,  $\rho_n = \rho_p$ )  $\rho_0 \sim 0.16 \text{ fm}^{-3}$  but differ substantially at high density. In other words, the properties of nuclear matter predicted from different models have analogous behavior around the saturation density but extremely different from each other at high density under  $\beta$ -equilibrium. The recently observed massive neutron stars, J1614-2230 (with mass of  $1.97 \pm 0.04M_{\odot}$ )<sup>12</sup> and J0348+0432 (with mass of  $2.01 \pm 0.04M_{\odot}$ ),<sup>13</sup> have provided a reliable information on the existence of massive compact stars. At present, the uncertainties are quite large in the radius of compact stars.<sup>14-17</sup> For example, using the pulse phase-resolved x-ray spectroscopy for pulsar J0437-4715 gives the radius of the compact star  $R \geq 11 \text{ km}$  with  $3\sigma$  uncertainty.<sup>17</sup> Furthermore, at high densities it is well known that there might be substantial population of heavy baryons (i.e. hyperons), because these become energetically favorable once the Fermi energy of neutrons reaches the order of their rest mass. Hence, it becomes quite necessary to include the hyperon matter in the study of highly dense compact objects. In the last few decades, a large number of systematic studies including hyperon in the nuclear matter (i.e., hyper-nuclear matter or hyperon matter) were carried out *before & after* the observation of the pulsars and their identification with the neutron stars.<sup>18-44</sup> Most of these works demonstrate that the mass of the compact stars is reduced by  $0.4M_{\odot}$  where contribution of the hyperon matter is included in the EoS, challenging the knowledge of the perceived modern mass.<sup>12,13</sup> Further, the inclusion of Fock channel in density dependent relativistic Hartree-Fock model rather effects substantially in softening the EoS for neutron stars.<sup>33-35</sup> This reduction in the mass of the compact stars due to hyperon matter in the EoS under  $\beta$ -equilibrium is known as *Hyperon Puzzle*.<sup>40-45</sup> The solution of this so called *Hyperon Puzzle* is not easy, it requires an additional contrivance that could provide a repulsion to make the EoS stiffer. At present, a few possible efforts have been

made in this directions such as strong hyperon–nucleon and/or hyperon–hyperon interactions;<sup>42,43,46,47</sup> the inclusion of three-body forces with one or more hyperons;<sup>48,49</sup> the appearance of other hadronic degrees of freedom and phase transition to deconfined quark matter<sup>50–56</sup> and considering differential rotating effects.<sup>57</sup> For more detailed on the *Hyperon Puzzle*, one can follow the recent review article of Refs.<sup>58,59</sup> and references therein.

It is well known that the theoretical  $Mass \sim Radius$  relation depends on the rotation frequency and also the presence of an exotic core in massive neutron star. Within present scenario, all neutron stars rotate and there are many millisecond pulsars with rotation frequency  $\geq 500$  Hz (10 accreting X-ray pulsars and 14 radio/gamma-ray pulsars). A radio millisecond pulsar B1937 + 21 rotating at frequency 641 Hz,<sup>60</sup> remained the most rapidly one for more than two decades and the discovery of pulsar J1748-2446ad with a faster rotating of frequency 716 Hz was announced in the year 2006.<sup>61</sup> Later observations of X-ray burst XTE J1739-285 noticed a formation of neutron star with an initial rotation frequency  $\nu_{in} \sim 1122$  Hz.<sup>62</sup> On the other hand the young pulsars has been known to have rotational frequency  $\leq 10$  Hz and in this category (according to the observations so far) PSR J0537-6910 is known to be the fastest with  $\nu_{max} \sim 62$  Hz.<sup>63</sup> In fact, the angular velocity distribution of a neutron star evolves to a uniform rotation within a very short time period in any supernova event.<sup>64,65</sup> Moreover, the sub-kHz frequencies are still too low to significantly affects the structure of massive neutron stars.<sup>6,66</sup> However, for rapid rotation i.e. the sub-millisecond pulsar with super-kHz frequencies, the rotation affects the massive neutron stars. Reviewing the works concerning the rapidly rotating stars in general relativity, there are few pioneering predictions, which have been observed by considering some of the sophisticated aspects of the neutron star: the nuclear equation of state, magnetic fields, magnetic field breaking and meridional flows etc. Here we give some of these references for such studies: Butterworth & Ipser (1976);<sup>67</sup> Komatsu *et al.* (1989);<sup>68</sup> Bonazzola *et al.* (1993);<sup>69</sup> Stergioulas & Friedman (1995);<sup>70</sup> Laarakkers & Poisson (1999);<sup>71</sup> Baumgarte *et al.* (2000);<sup>72</sup> Ansorg *et al.* (2002);<sup>73</sup> Birkel *et al.* (2010);<sup>74</sup> Krastev *et al.* (2008).<sup>41</sup> For more extensive global collection of literature, see Friedman & Stergioulas (2013).<sup>75</sup>

Besides the calculation performed by including the  $\omega$ - $\rho$  cross-coupling and quartic terms in the RMF softens the EoS to good agreement with the recent observed mass of compact stars.<sup>76–79</sup> In addition to that the generalized model having the low lying octet of baryons makes it difficult to obtain a neutron star mass greater than  $2.0M_{\odot}$ .<sup>43,44,77,79</sup> In continuation of our earlier work,<sup>79</sup> we here analyze the rotational attributes of neutron star with various hyperon-meson couplings within the framework of effective field theory motivated relativistic mean field model (E-RMF).<sup>43,76,79,80</sup> The degrees of freedom in this theory are nucleons interacting through the exchange of iso-scalar scalar  $\sigma$ -, iso-scalar vector  $\omega$ -, and iso-vector-vector  $\rho$ - meson fields. The chiral effective Lagrangian (i.e. the E-RMF formalism)<sup>37,76,80–88</sup> is the extension of the standard relativistic mean-field (RMF) the-

4 *M. Bhuyan*

ory<sup>28,36,89–96</sup> with the addition of nonlinear scalar-vector and vector-vector self-interaction, applying the naive dimensional analysis and the concept of naturalness at a given level of accuracy.<sup>37,76,80,81,85–88</sup> In particular, the motivation behind the present work is to investigate the axisymmetric hydrostatic equilibria of rotating neutron star and the effects of rotational profiles in the hyperon matter under  $\beta$ -equilibrium condition at high density. In other words, this present work will provide a relativistic mean field descriptions of the static and rotating (sub-millisecond to super-millisecond) compact star properties for various hyperon-meson couplings.

This paper is organized as follows: In Section II we discuss the theoretical setup for the relativistic mean field theory. The parametrization and values of their coupling constant are also included in this section. Section III–VI are assigned for the discussion of the results obtained from our calculation for the static and rotating compact stars. A short mathematical formulation for the equilibrium condition of static and rapidly rotating compact stars are also presented in the section IV & V. Finally, the summary and a brief conclusion are given in Section VII.

## 2. The relativistic mean-field theory

The elementary theory for strong interaction to represent the complete description of nuclear equation of state is quantum chromodynamics (QCD). At present, it is not conceivable to describe the complete picture of the hadronic matter due to its non-perturbative properties. Hence, one need to endorse the perception of effective field theory (EFT) at low energy, known as quantum hadrodynamics (QHD).<sup>89–91</sup> Now-a-days, the mean field treatment of QHD has been used widely to describe the properties of infinite nuclear matter<sup>76,87–89</sup> and finite nuclei.<sup>90–93,97–99</sup> In this theory, the nucleons are considered as Dirac particle, interact through the exchange of various mesons (i.e. iso-scalar scalar  $\sigma$ -, iso-scalar vector  $\omega$ -, iso-vector-vector  $\rho$ - and iso-vector-scalar  $\delta$ -mesons). The chiral effective Lagrangian (E-RMF) is proposed by Furnstahl, Serot and Tang,<sup>80,82,84,85,87,100</sup> the extension of the standard relativistic mean field model.<sup>89–96</sup> In E-RMF, the nonlinear Lagrangian is expanded with the increasing order of the fields along with their derivative up to 4<sup>th</sup> order of interaction under naive dimensional analysis<sup>83,84</sup> and the concept of naturalness.<sup>82,100,101</sup> In the interior of a neutron star, where the density is very high, other hadronic states are produced.<sup>40–45</sup> Thus, the considered model involves the full octet of baryons interacting through mesons. Finally, the truncated Lagrangian is given by

$$\begin{aligned} \mathcal{L} = & \sum_B \bar{\Psi}_B (i\gamma^\mu D_\mu - m_B + g_{\sigma B}\sigma) \Psi_B + \frac{1}{2}\partial_\mu\sigma\partial^\mu\sigma - \frac{1}{4}\Omega_{\mu\nu}\Omega^{\mu\nu} - \frac{1}{4}R_{\mu\nu}^a R^{a\mu\nu} \\ & - m_\sigma^2\sigma^2 \left( \frac{1}{2} + \frac{\kappa_3}{3!} \frac{g_{\sigma N}\sigma}{m_N} + \frac{\kappa_4}{4!} \frac{g_{\sigma N}^2\sigma^2}{m_N^2} \right) + \frac{1}{2} \left( 1 + \eta_1 \frac{g_{\sigma N}\sigma}{m_N} + \frac{\eta_2}{2} \frac{g_{\sigma N}^2\sigma^2}{m_N^2} \right) m_\omega^2\omega_\mu\omega^\mu \\ & + \frac{1}{2} \left( 1 + \eta_\rho \frac{g_{\sigma N}\sigma}{m_N} \right) m_\rho^2\rho_\mu^a\rho^{a\mu} + \frac{1}{4!}\zeta_0 g_{\omega N}^2 (\omega_\mu\omega^\mu)^2 + \sum_l \bar{\Psi}_l (i\gamma^\mu\partial_\mu - m_l) \Psi_l. \quad (1) \end{aligned}$$

The subscript  $B = n, p, \Lambda, \Sigma$  and  $\Xi$ , denotes baryons of  $m_B$ ,  $l$  stands for lepton ( $e^-$  &  $\mu^-$ ) of mass  $m_l$  and  $N$  for nucleons of mass  $m_N$ . The spin of all baryons is  $1/2$ . Here, the covariant derivative  $D_\mu$  is defined as

$$D_\mu = \partial_\mu + ig_{\omega B}\omega_\mu + ig_{\rho B}I_{3B}\tau^a\rho_\mu^a, \quad (2)$$

where, the term  $R_{\mu\nu}^a$ , and  $\Omega_{\mu\nu}$  are the field tensors,

$$R_{\mu\nu}^a = \partial_\mu\rho_\nu^a - \partial_\nu\rho_\mu^a + g_{\rho N}\epsilon_{abc}\rho_\mu^b\rho_\nu^c, \quad (3)$$

$$\Omega_{\mu\nu} = \partial_\mu\omega_\nu - \partial_\nu\omega_\mu. \quad (4)$$

Here,  $m_\sigma$ ,  $m_\omega$  and  $m_\rho$  are the masses for the baryon,  $\sigma$ -,  $\omega$ - and  $\rho$ -meson, respectively. From this Lagrangian, we derive the equation of motion and solve within mean field approximation self consistently. The obtained field equations for  $\sigma$ ,  $\omega$  and  $\rho$ -meson are given by

$$\begin{aligned} m_\sigma^2 \left( \sigma_0 + \frac{g_{\sigma N}\kappa_3}{2m_N}\sigma_0^2 + \frac{g_{\sigma N}^2\kappa_4}{6m_N^2}\sigma_0^3 \right) - \frac{1}{2}m_\rho^2\eta_\rho\frac{g_{\sigma N}}{m_N}\rho_0^2 \\ - \frac{1}{2}m_\omega^2 \left( \eta_1\frac{g_{\sigma N}}{m_N} + \eta_2\frac{g_{\sigma N}^2}{m_N^2}\sigma_0 \right) \omega_0^2 = \sum_B g_{\sigma B}\rho_{SB} \end{aligned} \quad (5)$$

$$m_\omega^2 \left( 1 + \eta_1\frac{g_{\sigma N}\sigma_0}{m_N} + \frac{\eta_2}{2}\frac{g_{\sigma N}^2\sigma_0^2}{2m_N^2} \right) \omega_0 + \frac{1}{6}\zeta_0g_{\omega N}^2\omega_0^3 = \sum_B g_{\omega B}\rho_B \quad (6)$$

$$m_\rho^2 \left( 1 + \eta_\rho\frac{g_{\sigma N}\sigma_0}{m_N} \right) \rho_{03} = \sum_B g_{\rho B}I_{3B}\rho_B \quad (7)$$

For a baryon species, the scalar density,  $\rho_{SB}$ , and baryon density ( $\rho_B$ ) are given as,

$$\rho_{SB} = \frac{2J_B + 1}{2\pi^2} \int_0^{k_B} \frac{M_B^*k^2 dk}{E_B^*} \quad (8)$$

$$\rho_B = \frac{2J_B + 1}{2\pi^2} \int_0^{k_B} k^2 dk, \quad (9)$$

where  $E_B^* = \sqrt{k^2 + m_B^{*2}}$  is the effective energy and  $J_B$  and  $I_{3B}$  are the spin and isospin projection of baryon, respectively. The quantity  $k_B$  is the Fermi momentum of the baryon, and  $m^* = m_B - g_{\sigma B}\sigma$  is the effective mass, which can solve self-consistently. Now, the pressure density  $\mathcal{P}$  and the energy density  $\mathcal{E}$  for a given baryon density are expressed as follow,

$$\begin{aligned} \mathcal{P} = \sum_B \frac{\gamma}{3(2\pi)^3} \int_0^{k_B} d^3k \frac{k^2}{E_B^*(k)} + \frac{1}{4!}\zeta_0g_{\omega N}^2\omega_0^4 + \frac{1}{2} \left( 1 + \eta_1\frac{g_{\sigma N}\sigma_0}{m_N} + \frac{\eta_2}{2}\frac{g_{\sigma N}^2\sigma_0^2}{m_N^2} \right) m_\omega^2\omega_0^2 \\ - \left( \frac{1}{2} + \frac{\kappa_3g_{\sigma N}\sigma_0}{3!m_N} + \frac{\kappa_4g_{\sigma N}^2\sigma_0^2}{4!m_N^2} \right) m_\sigma^2\sigma_0^2 + \frac{1}{2} \left( 1 + \eta_\rho\frac{g_{\sigma N}\sigma_0}{m_N} \right) m_\rho^2\rho_0^2 + \sum_l \mathcal{P}_l, \end{aligned} \quad (10)$$

6 *M. Bhuyan*

$$\begin{aligned} \mathcal{E} = & \sum_B \frac{\gamma}{(2\pi)^3} \int_0^{k_B} d^3k E_B^*(k) + \frac{1}{4!} \zeta_0 g_{\omega N}^2 \omega_0^4 + \frac{1}{2} \left( 1 + \eta_1 \frac{g_{\sigma N} \sigma_0}{m_N} + \frac{\eta_2}{2} \frac{g_{\sigma N}^2 \sigma_0^2}{m_N^2} \right) m_{\omega}^2 \omega_0^2 \\ & + \left( \frac{1}{2} + \frac{\kappa_3 g_{\sigma N} \sigma_0}{3! m_N} + \frac{\kappa_4 g_{\sigma N}^2 \sigma_0^2}{4! m_N^2} \right) m_{\sigma}^2 \sigma_0^2 + \frac{1}{2} \left( 1 + \eta_{\rho} \frac{g_{\sigma N} \sigma_0}{m_N} \right) m_{\rho}^2 \rho_0^2 + \sum_l \mathcal{E}_l. \end{aligned} \quad (11)$$

Here, the constant  $\gamma = 2$  is known as spin degeneracy parameter. The pressure density and energy density contribution from leptons are represented by  $\mathcal{P}_l$  and  $\mathcal{E}_l$ , respectively.

### 3. Nuclear matter at saturation density

We know that the infinite nuclear matter is an essential system for the investigation of physical quantities relevant to heavy nuclei and compact objects like a neutron star. Furthermore, at saturation density, the binding energy per particle, pressure density, symmetry energy and compressibility are well established physical quantities from the empirical and experimental observation. For general idea, the results obtained within E-RMF at saturation density  $\rho_0$  are listed in Table 1, which are consistent with the recent constrained values except the slope parameter  $L_{sym}$ .<sup>102</sup> Following the work of Lattimer *et al.*,<sup>102</sup> the values of  $L_{sym}$  within G2 force is a little overestimated compared to their recent constraint limit. We have also shown results for the energy density and the pressure density as a function of baryon density using Eqs. (10 & 11) for our calculations for G2 force in the left panel and right panel of Fig. 1, respectively. The obtained results are compared with the M3Y-P5,<sup>103</sup> DBHF<sup>104</sup> and the realistic calculation done by Akmal *et al.*<sup>8</sup> In the right panel of Fig. 1, we have also compared the results from our calculation with DBHF<sup>105</sup> and DD-F<sup>106</sup> predictions. The shaded areas within solid and broken line correspond to the empirical results extracted from HIC<sup>107</sup> and  $K^+$  production data,<sup>108</sup> respectively for comparison. From the figure, one can find that the obtained results from our calculation agree well with all others theoretical predictions and also with the empirical data. It is to be noted that in G2 force, the quartic term of the  $\omega$ -meson and cross coupling of the scalar field plays the major role in the softening of the EoS at high density with a reasonable compressibility.<sup>76</sup> Being extension to the previous works,<sup>79</sup> the aim is to study the dependence of neutron star properties with an exotic core and the imprint of rotation on the mass-equatorial radius relation and the stability of rotating configurations.

### 4. Baryonic matter in $\beta$ -equilibrium

In the interior of neutron stars, the neutron chemical potential goes beyond the total mass of the proton and electron. In other words, a probabilistic neutron star composition of neutron star is asymmetric matter with an admixture of electrons rather than pure neutron matter. Further, the density is expected to be high enough ( $\sim 7-8\rho_0$ ) in the core of the neutron star, that undergoes a transition to other

Table 1. The mass of different mesons, the coupling constant, and the nuclear matter saturation properties for E-RMF (G2) force parameter. The masses are in MeV.

Meson Mass	Coupling Constant	Nuclear Matter Properties
$m_\sigma = 520$	$g_\sigma = 0.83522$	$m^*/m = 0.66$
$m_\omega = 782$	$g_\omega = 1.01560$	$\rho_0 = 0.15$
$m_\rho = 770$	$g_\rho = 0.75467$	$\varepsilon(\rho_0) = -16.1$
	$\kappa_3 = 3.2467$	$K_0 = 214.7$
	$\kappa_4 = 0.63152$	$E_{\text{sym}} = 36.4$
	$\zeta_0 = 2.6416$	$L_{\text{sym}} = 100.7$
	$\eta_1 = 0.64992$	
	$\eta_2 = 0.10975$	
	$\eta_\rho = 0.3901$	

Table 2. The hyperon-meson coupling ratios for baryon octet family for four different parametrisation. The maximum masses and the corresponding radii are obtained for static and stationary rotating compact star at Keplerian frequency for different EoSs. The quantities given within the bracket are the mass and radius of the neutron star without hyperons.

	Set 1 <sup>25</sup>	Set 1a <sup>25</sup>	Set 2 <sup>117</sup>	Set 2a <sup>118</sup>
$x_{\sigma\Lambda}$	0.4800	0.5800	0.6104	0.6106
$x_{\sigma\Sigma}$	0.4800	0.5800	0.6104	0.4046
$x_{\sigma\Xi}$	0.0000	0.5800	0.6104	0.3195
$x_{\omega\Lambda}$	0.5600	0.6600	0.6666	0.6666
$x_{\omega\Sigma}$	0.0000	0.0000	0.6666	0.6666
$x_{\omega\Xi}$	0.0000	0.3333	0.6666	0.3333
$x_{\rho\Lambda}$	0.0000	0.7500	0.6104	1.0000
$x_{\rho\Sigma}$	0.0000	0.0000	0.6104	1.0000
$x_{\rho\Xi}$	0.0000	2.0000	0.6104	1.0000
Static star				
$M/M_\odot$	1.43 (2.04)	1.48 (2.04)	1.51 (2.04)	1.54 (2.04)
$R$	11.02 (11.02)	11.02 (11.02)	11.03 (11.02)	11.03 (11.02)
Rotating star				
$M/M_\odot$	2.11 (2.43)	2.14 (2.43)	2.17 (2.43)	2.19 (2.43)
$R$	13.35 (13.28)	13.35 (13.28)	13.36 (13.28)	13.36 (13.28)

hadronic states i.e the low lying octet of baryons ( $\Lambda^0$ ,  $\Sigma^0$ ,  $\Sigma^+$ ,  $\Sigma^-$ ,  $\Xi^0$ , and  $\Xi^-$ ) apart from the nucleons are produced.<sup>21, 83, 109, 110</sup> For stars, the strongly interacting particles are baryons, the composition is determined by the requirements of charge neutrality and  $\beta$ -equilibrium conditions under the weak processes,<sup>85, 111, 112</sup>  $B_1 \rightarrow B_2 + l + \bar{\nu}_l$  and  $B_2 + l \rightarrow B_1 + \nu_l$ . Here,  $B_1$  &  $B_2$ ,  $l$ ,  $\nu$  and  $\bar{\nu}$  are the baryons, leptons, neutrino and anti-neutrino respectively. After deleptonization, the charge neutrality condition yields,

$$q_{\text{tot}} = \sum_B q_B k_B^3 / (3\pi^2) + \sum_{l=e,\mu} q_l k_l^3 / (3\pi^2) = 0. \quad (12)$$

Here, the  $q_B$  and  $q_l$  correspond to the electric charge of baryon ( $B$ ) and lepton species ( $l$ ), respectively. Since the time scale of a star is effectively infinite compared

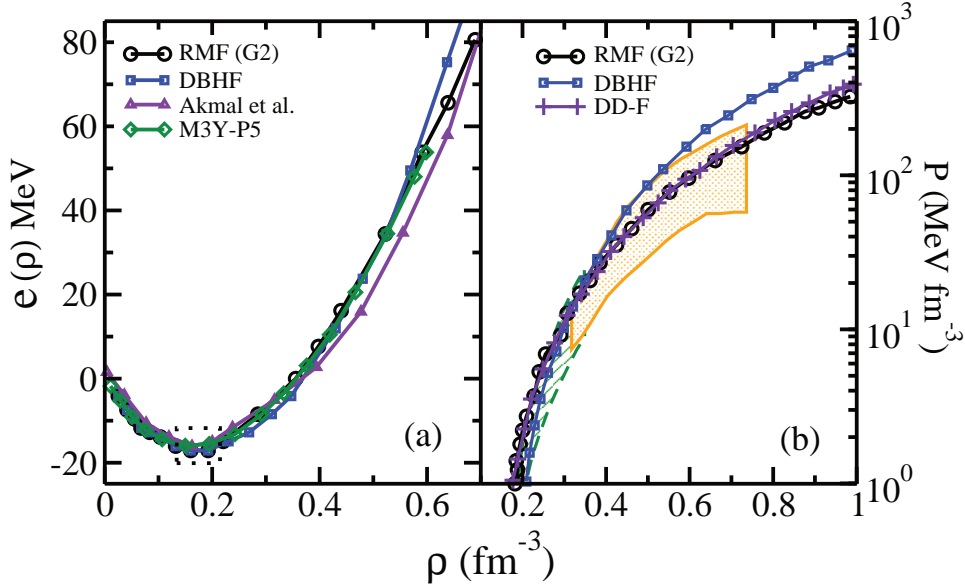


Fig. 1. (Color online) (a) The obtained energy per particle as a function of density from G2 force is compared with M3Y-P5,<sup>103</sup> DBHF,<sup>104</sup> and the realistic calculation.<sup>8</sup> (b) The obtained pressure density as a function of density from G2 force is compared with DBHF<sup>105</sup> and DD-F.<sup>106</sup> The areas within solid and broken line correspond to the results extracted from HIC<sup>107</sup> and  $K^+$  production data,<sup>108</sup> respectively. See text for details.

to the weak interaction time scale, the strangeness quantum number is therefore not conserved in a star. The net strangeness is determined by the condition of  $\beta$ -equilibrium, which for baryon is then given by  $\mu_B = b_B \mu_n - q_B \mu_e$ , where  $\mu_B$  is the chemical potential of baryon number  $b_B$ . Thus the chemical potential of any baryon can be obtained from the two independent chemical potentials  $\mu_n$  and  $\mu_e$  of neutrons and electrons, respectively. Hence, the equilibrium composition of the star is obtained by solving the set of equations for the chemical potential in conjunction with the charge neutrality condition in Eq. 12 at a given baryon density. On the basis of the quark model, one can assume that the hyperons interact with the mesons in two distinct modes by permitting the mixing and breaking of SU(6) symmetry, keeping nuclear coupling constant intact.<sup>25,113–118</sup> We have used these two methods of parametrisations: (i) same coupling ratios as assumed by the quark model<sup>25,115,116</sup> (see Set 1 & 1a of Table 2) and (ii) different couplings strength for different baryons<sup>114,117,118</sup> (see Set 2 & 2a of Table 2) to deals with the octet of baryons in the EoS of compact star. The adopted hyperon-meson coupling ratios and their values for the present studies are listed in Table 2.

By imposing the above conditions on the Eqs. (10,11), we have self consistently calculated the energy density  $\mathcal{E}$  and pressure density  $\mathcal{P}$  of hyper-nuclear star matter as a function of baryon density. The results obtained for nuclear (i.e., proton and



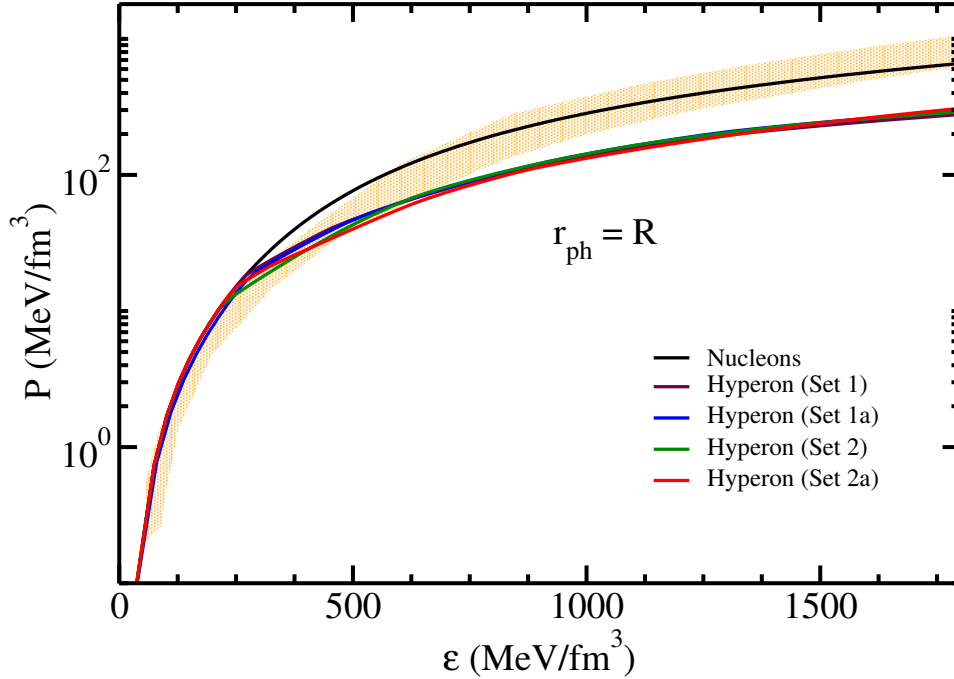


Fig. 2. (Color online) The equation of states obtained for nuclear and hyperon matter under charge neutrality as well as the  $\beta$ -equilibrium condition from G2 force are compared with the empirical data (shaded area in the graph) by Steiner *et al.* for  $r_{ph} = R$  with the uncertainty of  $2\sigma$ .<sup>120</sup>

neutron) and the octet system (i.e. proton, neutron,  $\Lambda^0$ ,  $\Sigma^0$ ,  $\Sigma^+$ ,  $\Sigma^-$ ,  $\Xi^0$ , and  $\Xi^-$ ) are shown in Fig. 2. In those curves, there are five EoSs for compact star, one from nucleonic matter and four from hyper-nuclear matter for various hyperon-meson coupling ratios (given in Table 2). From the figure, it is clearly noticed that the EoS from the nucleonic matter is a little stiffer compared to the hyperon matter at high density. In other words, the inclusion of hyperons into the compact star, gives a softer EoS as compared to the nucleonic matter with respect to the baryon density. Comparison with the empirical data for  $r_{ph} = R$  with the uncertainty  $2\sigma$  of Steiner *et al.*<sup>119,120</sup> (shaded region) is also depicted. Here  $R$  and  $r_{ph}$  are for the neutron radius and the photospheric radius, respectively. More care inspection to the figure shows that the EoS for nuclear system agrees well with the empirical data throughout the densities, but deviates a little for hyperon matter at high density. For example, the EoS obtained from the baryon octet family coincides with the empirical values up to the density  $\sim 6\rho_0$ , then it becomes a little softer compared to empirical values. Hence, one can interpret that the inclusion of hyperon matter to the nucleon system makes the neutron star EoS softer as shown in the figure, which is consistent with the other theoretical predictions.<sup>25,33–37,40–53,58,59,113–118</sup>

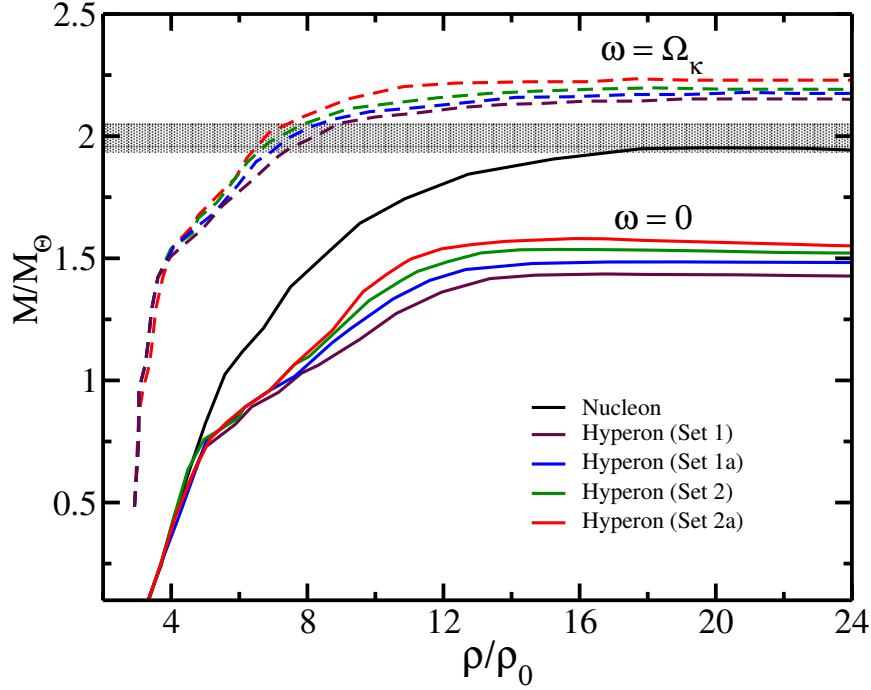


Fig. 3. (Color online) The obtained static (solid line) and rotational (dashed line) compact star mass for nuclear and hyper-nuclear matter as a function of baryon density are given along with the recent mass observations.<sup>12,13</sup> See text for details.

### 5. Stellar equations for static and rotating neutron star

The structure of a spherically symmetric and static compact star, consisting of relativistic matter modeled as perfect fluid, can be studied in term of energy density  $\mathcal{E}$  and the pressure density  $\mathcal{P}$  as a function of baryon density using Tolman-Oppenheimer-Volkoff equations.<sup>2,3</sup> The general form of the TOV equation is given by:

$$\frac{d\mathcal{P}}{dr} = -\frac{G}{r} \frac{[\mathcal{E} + \mathcal{P}] [M + 4\pi r^3 \mathcal{P}]}{(r - 2GM)}, \quad (13)$$

$$\frac{dM}{dr} = 4\pi r^2 \mathcal{E}, \quad (14)$$

where  $G$  and  $M(r)$  are the gravitational constant and the enclosed gravitational mass of radius  $r$ , respectively. For a given value of  $\mathcal{P}$  and  $\mathcal{E}$ , these equations can be integrated from the origin as an initial value problem for a given choice of central energy density. The value of  $r(=R)$ , where the pressure vanishes defines the surface of the star.

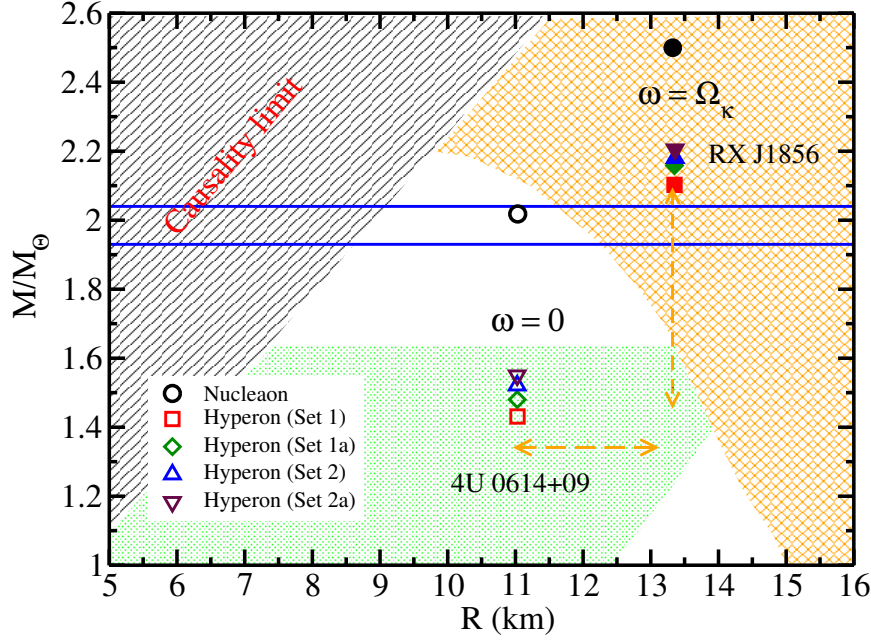


Fig. 4. (Color online) The obtained mass and radius trajectories nuclear and hyper-nuclear matter of static and rotational compact stars are compared with the recent mass observational datas<sup>12,13</sup> (the region between two solid horizontal blue line). The dashed orange vertical and horizontal lines are stands for the shift of mass and radius respectively due to the inclusion of rotational profile to the EoSs of compact star. The mass-radius constraints from thermal radiation of isolated neutron star RX J1856<sup>106</sup> (orange hatched area) and from QPOs in the LMXBs 4U 0614+09<sup>122</sup> (green hatched area) are given for constraining to the EoSs of compact stars. See text for more details.

As we know, the fast rotating relativistic compact stars are sensitive to the stellar mass and to the equations of state at high density under  $\beta$ -equilibrium. Further, the rotational instabilities can produce gravitational waves, the detection of which would initiate a new field of observational asteroseismology of relativistic stars.<sup>121</sup> Many interesting phenomena are studied from several independent numerical codes for obtaining accurate picture of rotating neutron stars in full general relativistic framework. The metric of the space time for a realistic configurations of an axis-symmetric and stationary rotating compact star in spherical polar coordinate is given by:<sup>68,71</sup>

$$ds^2 = -e^{2\nu} dt^2 + e^{2\alpha} (dr^2 + r^2 d\theta^2) + e^{2\beta} r^2 \sin^2 \theta (d\phi - \omega dt)^2. \quad (15)$$

Here,  $(r, \theta, \text{ and } \phi)$  are the spherical polar coordinates and the metric potentials  $\nu, \alpha, \beta, \omega$  are functions of  $r$  and  $\theta$  only.<sup>70,71</sup> In the limit of perfect fluid, the energy momentum tensor can be given as,

$$T^{\mu\nu} = P g^{\mu\nu} + (P + \mathcal{E}) u^\mu u^\nu, \quad (16)$$

12 *M. Bhuyan*

where  $\varepsilon$ ,  $\mathcal{P}$ , and  $u^\mu$  are the total energy density, the pressure density and the four velocity, respectively.<sup>70,75</sup> Here, one should follow the three basic equations: (i) the Einstein's equation for the metric potentials

$$G_{\mu\nu} = 8\pi T_{\mu\nu};$$

(ii) the rest mass conservation

$$\nabla_\mu (\rho u^\mu) = 0;$$

and (iii) the stress energy conservation

$$\nabla_\nu T^{\mu\nu} = 0; \quad (17)$$

see Ref.,<sup>68</sup> for detailed mathematical expressions. Furthermore the Einstein's equation is split into four component for the potentials and the four velocity as,

$$u^\mu = \frac{e^{-\nu}}{\sqrt{1-v^2}}(1, 0, 0, \Omega). \quad (18)$$

Here,  $v$  is the spatial linear velocity with respect to an observer with zero angular momentum,

$$v = e^{\beta-\nu} r \sin \theta (\Omega - \omega). \quad (19)$$

Now, we can use the limit on the maximum rotation, by the onset of mass shedding from the EoS of the compact star. Here, we have used the geometrized units,  $c = G = 1$ . For calculation of the rotational compact star properties like mass, radius and rotational frequency, we have used the well known rotational neutron star (RNS) code, which is written by Stergioulas & Friedman.<sup>70</sup>

The calculated maximum mass  $M$  and the radius  $R$  for the static nuclear and hyperon stars are obtained from the well-known TOV equations using the EoSs of E-RMF. The estimated results for the maximum mass as a function of density are compared with the observational data from pulsars J1614-2230 and J0348+0432,<sup>12,13</sup> shown in Fig. 3. We have shown the maximum mass and radius trajectory for the static and rotating compact star in Fig. 4. The dashed orange vertical and horizontal lines in the figure stands for the shift of mass and radius respectively due to the inclusion of rotational profile to the EoSs of compact star (will discuss in the preceding paragraph). The mass-radius constraints from thermal radiation of isolated neutron star RX J1856<sup>106</sup> (orange hatched area) and from QPOs in the LMXBs 4U 0614+09<sup>122</sup> (green hatched area) are given for constraining the EOSs of compact stars. Ensuing these recent observations,<sup>12,13,106,122</sup> it is clearly illustrated that the maximum mass predicted by any theoretical models should reach or near the limit  $\sim 2.0M_\odot$ , which is consistent with our present prediction from the EoS of nucleonic matter compact star. But, the mass reduced somewhat by inclusion of hyperon matter to the EoSs under  $\beta$ -equilibrium conditions. In other words, the maximum mass obtained from nuclear matter EoS is reduced by  $\sim 0.4M_\odot$  in presence of hyperon matter core. For example, the mass predicted from the nuclear and hyper-nuclear matter are  $\sim 2.1M_\odot$  and  $\sim 1.5M_\odot$ , respectively for static compact

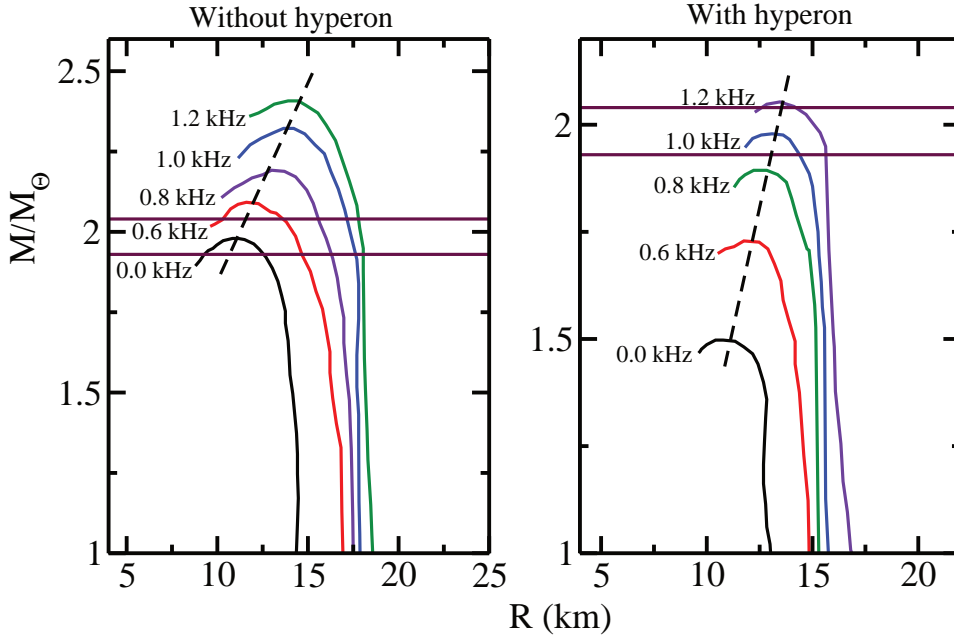


Fig. 5. (Color online) The gravitational mass *vs.* radius configuration for EoS of nuclear and hyperon matter compact stars with constant rotational frequency. The rotational frequency is labeled for each trajectory. The horizontal line in each panel represent the recent mass observation<sup>12,13</sup> are given for an ideal reference for the mass and radius. See text for more details.

star using the TOV equation (see Figs. 3 & 4). Hence, one can easily contend that the predicted maximum mass from the hyperon matter EoSs is underestimated to the recent mass observations,<sup>12,13</sup> which is the well known *Hyperon Puzzle*. It is worth mentioning that the results obtained from our calculations are in consistent with the recent theoretical predictions.<sup>25, 33–37, 40–53, 58, 59, 113–118</sup> Furthermore, there is no significant precise information regarding the constraint on the radius  $R$  of the compact star. Hence in all cases, the radius of the neutron star corresponding to the maximum mass is within the range of  $\sim 12$  km, which satisfy the standard value as predicted in the Ref.<sup>123,124</sup> for 214 Skyrme-Hartree-Fock forces.

The stationary configurations of a compact star rotating at a given rotational frequency  $\omega$  forms an one-parameter family characterized by central density  $\rho_c$ , with limitation of two instabilities in the mass *vs.* equatorial radius plane. For the high central density, the axis-symmetric perturbation makes it unstable, as a result the star collapse into a Kerr Black hole.<sup>125</sup> In this section we performed the calculations for Mass *vs.* radius relations of very fast rotating (the Keplerian frequency  $\omega = \Omega_k$ ) for five different EOSs of compact star using RNS equations. The obtained results are given along with the non-rotating compact star properties in Fig. 3 & 4. From the figures, it is clearly noticed that the rotational profile for

the EoS at  $\omega = \Omega_k$  brings a mass increase by  $\sim 0.5M_\odot$  and radius by  $\sim 2$  km (see Figs. 3 & 4). In other words, the maximum gravitational mass and radius for a given EoS is enhanced by  $\sim 0.5M_\odot$  and  $\sim 2$  km, respectively for a compact star with Keplerian frequency. Quantitatively, the mass predicted using EoS of hyperon matter of certain coupling ratio are  $\sim 1.5$  (for static compact star using TOV equations) and  $\sim 2.0$  for stationary rotation (using RNS equations). The obtained results for the rotating neutron star properties are consistent with the works by Haensel *et al.*<sup>44</sup> The crucial question from the observational point of view is which the instability with respect to oscillations determine the bound state of the compact stars. In order to answer this question, we have calculated the gravitational mass-radius trajectories for a broad range of sub-millisecond frequencies, 0.6–1.4 kHz of uniformly rotating compact stars. The obtained results are displayed in Fig. 5 along with the recent mass observation.<sup>12,13</sup> The left and right panel of the figure are corresponding to the EoS of nuclear and hyperon matter compact star, respectively. Here, we give the results of mass-shedding for a given rotational frequency for only one EoS of hyperon matter obtained from Set 2a<sup>118</sup> (see Table 2), as a example. We have also found similar results for all other hyperon matter EoSs obtained by using the various hyperon-meson couplings listed in Table 2. In the figure, we have only shown the mass-shedding points for each frequency of millisecond compact stars with respect to axis-symmetric stationary rotation. From the figure, it is clear that the mass and the radius increases monotonically with the rotational frequency. Instability with respect to the mass-shedding from the equator implies that for a specific rotational frequency the gravitational mass and radius should be smaller than the maximum mass at Keplerian limit. Hence, one can conclude that the properties of a compact star are influenced with the rotational frequency of the compact star but the mass of the hyperon star can only reach to the recent mass prediction at Keplerian frequency. Nevertheless, both features i.e. hyperon matter in the compact star and the rotation profile are of great practical importance and interest. In principle, they are very useful for selecting a perfect EoS to constrain the mass measurement and is simultaneously able to work for a wide range of rotational frequencies.

## 6. Composition of nuclear matter

In the above, we have mentioned that there are two different ways to incorporate the hyperon-meson coupling ratio into account: (i) constant coupling ratios as assumed by the quark model<sup>25,115</sup> (i.e Set 1 & 1a of Table 2) and (ii) variable couplings for different baryons<sup>117,118</sup> (Set 2 & 2a of Table 2). The results obtained for the yield as a function of density using these coupling ratios are shown in Fig. 6. The left and right panel of the figure represents the prediction from the constant and variable couplings, respectively. Furthermore, the solid and dashed lines in each panel stand for the two sets of coupling for a specific approach in the hyperon-meson interactions. From the figure, it is easily noticed that the  $\Sigma^-$  is generated

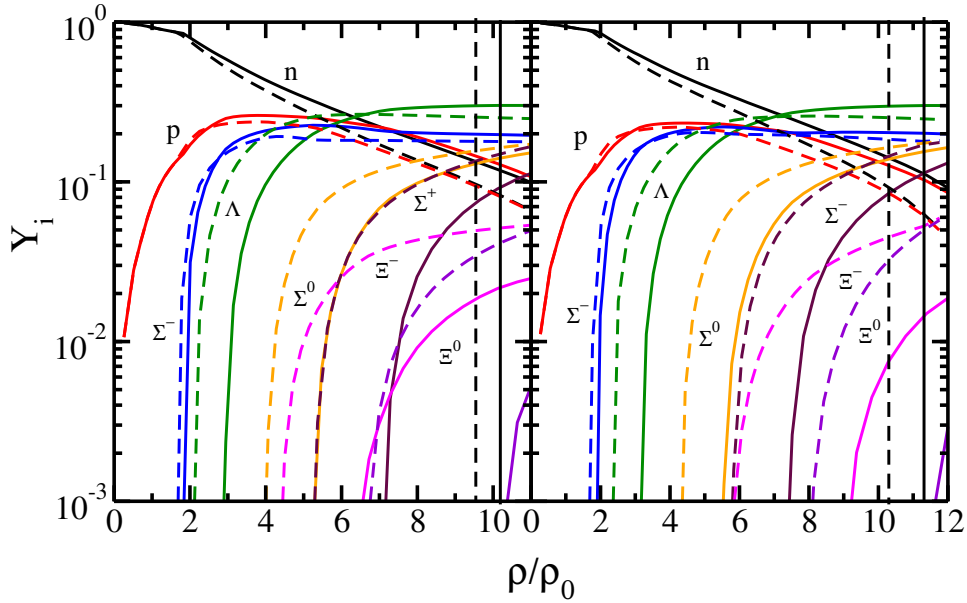


Fig. 6. (Color online) The particle fractions in hyperon matter as a function of density. Left panel, for constant coupling ratios<sup>25,115</sup> (Set 1 & 1a of Table 2) and Right panel, for variable coupling ratios<sup>117,118</sup> (Set 2 & 2a of Table 2). The vertical black lines (solid and dashed) in each panel for the central density of the neutron star at the maximum mass. See text for more details.

at  $\rho_B \sim 2.0\rho_0$  and its fraction increases rapidly to a saturation at  $\rho_B \sim 3.1\rho_0$ . Similarly, the  $\Lambda$ -hyperon generated at  $\sim 2.1\rho_0$  and the yield becomes constant at  $\sim 5.1\rho_0$ . From the figure, one can clearly notice that the yields for the two coupling ratios for each (constant & variable) approach have almost similar predictions. A careful investigation between two methodologies are found to differ a little from each other for the yields with respect to density. In other words, the procreation of hyperons as a function of density are altered a little for two approaches. Hence, one can conclude that the yields are marginally dependent on coupling ratios.

## 7. Summary and Conclusions

In the present study, we applied an effective field theory motivated relativistic mean field approach to the nuclear matter, where we investigated the influence of hyperon matter and the rotational profile on the properties of the compact star. We have generated four EoSs for the hyperon matter stars using various hyperon-meson coupling ratios. All the predicted EoSs for the hyperon stars have produced a maximum mass  $\sim 1.5M_\odot$ , which is lower compared to the recent star observation data.<sup>12,13</sup> The maximum radii corresponding to the masses are located in the range of 11–13 km. The influence of hyperon in the present study are consistent with the predictions of other theoretical calculations,<sup>25,40–53,58,59,113–118</sup> both early and the recent

ones in their mass spectrum under charge neutrality and  $\beta$ -equilibrium conditions. In continuation to the it Hyperon Puzzle, we have included the rotational profile under axis-symmetric constant rotation with Keplerian frequency into account using rotational star equation, which increase the mass of the compact star by  $\sim 0.5$  solar mass in magnitude as compared to the static case. In other words, the EoSs of hyperon matter along with the rotational profile at Keplerian limit predict the extreme mass  $\sim 2.1M_{\odot}$ , which are in good agreement with the late observation.<sup>12,13</sup> Furthermore, we have also calculated the mass-shedding for a given EoS for rotational frequency sequences of uniformly rotating compact stars. We found that the mass and the radius are increased monotonically with the rotational frequency for millisecond pulsar. Instability with respect to the mass-shedding from the equator implies that for a specific rotational frequency the gravitational mass and radius should be smaller than the maximum mass at Keplerian limit. From the above analysis, one can conclude that, the properties of a compact star are influenced with the rotational frequency but the mass of the hyperon star can only reach to the recent mass prediction at Keplerian frequency. In other words, the inclusion of rotational profiles to the neutron stars EoSs are not a full phase solution for the *Hyperon Puzzle*. Hence, it is important to consider other features along with the rotational profile in predictions of the hyperon star properties. In principle, the constituent of the core of the compact star is very useful for selecting a perfect EoS to constrain the mass measurement and is simultaneously able to work for a wide range of rotational frequencies. In summary, the present study is useful in the admiration of the expectation of static and stationary rotating hyper-nuclear compact stars at high density.

### Acknowledgments

This work has been supported by the 973 Program of China (Grant No. 2013CB834400), the NSF of China (Grants No. 11120101005, No. 11275248, and No. 11525524), the Chinese Academy of Sciences (Grant No. KJCX2-EW-N01) and the FAPESP Project No. 2014/26195-5 and and by the CNPq - Brasil.

### References

1. W. Baade and F. Zwicky, *Phys. Rev.* **46** (1934) 76.
2. R. Tolman, *Phys. Rev.* **55** (1939) 364.
3. J. Oppenheimer and G. Volkoff, *Phys. Rev.* **55** (1939) 374.
4. S. Chandrasekhar, *Astrophys. J.* **74** (1931) 81.
5. P. Ghosh, *Rotation and Accretion Powered Pulsars*, World Scientific, Singapore, (2007).
6. P. Hansel, A. Y. Potekhin and D. G. Yakovlev, **Vol-326** of *Astrophysics and Space Science Library*, (2007) (<http://www.astroscu.unam.mx/neutrones/home.html>).
7. J. R. Stone, J. C. Miller, R. Koncewicz, P. D. Stevenson and M. R. Strayer, *Phys. Rev. C* **68** (2003) 034324.
8. A. Akmal, V. R. Pandharipande and D. G. Ravenhall, *Phys. Rev. C* **58** (1998) 1804.
9. J. D. Walecka, *Theoretical Nuclear and Subnuclear Physics*, Imperial College and World Scientific, London and Singapore, (2004), ISBN 981-238-898-2.



10. S. L. Shapiro and S. A. Teukolsky, *Black holes, white dwarfs and neutron stars: The Physics of compact objects*, John Wiley and Sons, New York, (1983).
11. F. Weber, *Pulsars as Astrophysical Laboratories for Nuclear and Particle Physics*, Inst. Phys. Publishing, Bristol, (1999).
12. P. B. Demorest, T. Pennucci, S. M. Ransom, M. S. E. Roberts, and J. W. T. Hessels, *Nature (London)* **467** (2010) 1081.
13. J. Antoniadis et al., *Science* **340** (2013) 6131.
14. S. Guillot, R. E. Rutledge, and E. F. Brown, *Astrophys. J.* **732** (2011) 88.
15. T. Güver, P. Wroblewski, L. Camarota, and F. Özel, *Astrophys. J.* **719** (2010) 1807.
16. D. K. Galloway and N. Lampe, *Astrophys. J.* **747** (2012) 75.
17. S. Bogdanov, *Astrophys. J.* **762** (2013) 96.
18. V. A. Ambartsumyan and G. S. Saakyan, *Astron. Zh.* **37** (1960) 193.
19. S. A. Moszkowski, *Phys. Rev. D* **9** (1974) 1613.
20. N. K. Glendenning, *Phys. Lett. B* **114** (1982) 392.
21. N. K. Glendenning, *Astrophys. J.* **293** (1985) 470.
22. N. K. Glendenning, *Zeitschr. Phys. A* **326** (1987) 57.
23. F. Weber and M. K. Weigel, *Nucl. Phys. A* **493** (1989) 549.
24. J. I. Kapusta and K. A. Olive, *Phys. Rev. Lett.* **64** (1990) 13.
25. J. Ellis, J. I. Kapusta, and K. A. Olive, *Nucl. Phys. B* **348** (1991) 345.
26. P. J. Ellis, R. Knorren, and M. Prakash, *Phys. Lett. B* **349** (1995) 11.
27. J. Schaffner and I. N. Mishustin, *Phys. Rev. C* **53** (1996) 1416.
28. H. Huber, F. Weber, M. K. Weigel and Ch. Schaab, *Int. J. Mod. Phys. E* **07** (1998) 301.
29. A. Sedrakian, *Prog. Part. Nucl. Phys.* **58** (2007) 168.
30. S. Balberg, I. Lichtenstadt, and G. B. Cook, *Astrophys. J. Suppl.* **121** (1999) 515.
31. B.-Y. Sun, W.-H. Long, J. Meng, and U. Lombardo, *Phys. Rev. C* **78** (2008) 065805.
32. H.-J. Schulze and T. Rijken, *Phys. Rev. C* **84** (2011) 035801.
33. W.-H. Long, B.-Y. Sun, K. Hagino, and H. Sagawa, *Phys. Rev. C* **85** (2012) 025806.
34. N. B. Zhang, B. Qi, S.-Y. Wang, S. L. Ge, B.-Y. Sun, *Int. J. Mod. Phys. E* **22** (2013) 1350085.
35. B. Qi, N.-B. Zhang, S.-Y. Wang, and B.-Y. Sun, *Chin. Phys. Lett.* **32** (2015) 112101.
36. Y. Lim, C. H. Hyun, K. Kwak, and C.-H. Lee, *Int. J. Mod. Phys. E* **24** (2015) 1550100.
37. S. K. Biswal, B. Kumar, and S. K. Patra, *Int. J. Mod. Phys. E* **25** (2016) 1650090.
38. D. Logoteta, I. Vidaña, C. Providência, A. Polls, and I. Bombaci, *J. Phys. Conf. Ser.* **342** (2012) 012006.
39. X.-F. Zhao, and H.-Y. Jia, *Phys. Rev. C* **85** (2012) 065806.
40. S. K. Dhiman, Raj Kumar, and B. K. Agrawal, *Phys. Rev. C* **76** (2007) 045801.
41. Plamen G. Krastev, Bao-An Li, and Aaron Worley, *Astrophys. J.* **676** (2008) 1170.
42. M. Oertel, C. Providência, F. Gulminelli and Ad R. Raduta, *J. Phys. G: Nucl. Part. Phys.* **42**, (2015) 075202.
43. B. K. Sharma, M. Centelles, X. Viñas, M. Baldo, and G. F. Burgio, *Astron. Astrophys.* **103** (2015) 584.
44. P. Haensel, M. Bejger, M. Fortina, and L. Zdunik, *Eur. Phys. J. A* **52** (2016) 59.
45. I. Bombaci, arXiv:1601.05339, (2016).
46. I. Bednarek, P. Haensel, J. L. Zdunik, M. Bejger, and R. Manka, *Astron. Astrophys.* **157** (2012) 543.
47. K. A. Maslov, E. E. Kolomeitsev, and D. N. Voskresensky, *Phys. Lett. B* **748** (2015) 369.
48. Y. Yamamoto, T. Furumoto, N. Yasutake, and T. A. Rijken, *Phys. Rev. C* **90** (2014) 045805.

18 *M. Bhuyan*

49. D. Lonardonì, A. Lovato, S. Gandolfi, and F. Pederiva, *Phys. Rev. Lett.* **114** (2015) 092301.
50. A. Drago, A. Lavagno, G. Pagliara, and D. Pigato, *Phys. Rev. C* **90** (2014) 065809.
51. M. Alford, D. Blaschke, A. Drago *et al.*, *Nature*, **445** (2007) E7.
52. T. Klahn, R. Aastowiecki, and D. B. Blaschke, *Phys. Rev. D* **88** (2013) 085001.
53. J. L. Zdunik, and P. Haensel, *Astron. Astrophys.* **551** (2013) 61.
54. D. E. Alvarez-Castillo, and D. Blaschke, *Phys. Part. Nucl.* **46** (2015) 846.
55. S. Benic, D. Blaschke, D. E. Alvarez-Castillo, T. Fischer, and S. Typel, *Astron. Astrophys.* **577** (2015) A40.
56. M. Bejger, D. Blaschke, P. Haensel, J. L. Zdunik, and M. Fortin, *Astron. Astrophys.* **600** (2017) A39.
57. D. Gondek-Rosińska, I. Kowalska, L. Villain, M. Ansorg, and M. Kucaba, *Astrophys. J.* **837** (2017) 58.
58. D. Chatterjee, and I. Vidana, *Eur. Phys. J. A* **52** (2016) 3.
59. L. Tolos, M. Centelles, and A. Ramos, *Astrophys. J.* **834** (2017) 3.
60. D. C. Backer, S. R. Kulkarni, C. Heiles *et al.*, *Nature* **300** (1982) 615.
61. J. W. T. Hessels, S. M. Ransom, I. H. Stairs, P. C. C. Freire, V. M. Kaspi, and F. Camilo, *Science* **311** (2006) 1901.
62. P. Kaaret, Z. Prieskorn, J. J. M. in 't Zand, S. Brandt, N. Lund, S. Mereghetti, D. Götz, E. Kuulkers, and J. A. Tomsick, *Astrophys. J.* **657** (2007) L97.
63. F. E. Marshall *et al.*, *Astrophys. J.* **603** (2004) 682.
64. N. Andersson, *Astrophys. J.* **502** (1998) 708.
65. N. Andersson, K. D. Kokkotas, *Int. J. Mod. Phys. D* **10** (2001) 381.
66. S. L. Shapiro, S. A. Teukolsky, I. Wasserman, *Astrophys. J.* **272** (1983) 702.
67. E. M. Butterworth, and J. R. Ipser, *Astrophys. J.* **204** (1976) 200.
68. H. Komatsu, Y. Eriguchi, and I. Hachisu, *Mon. Not. R. Astron. Soc.* **237** (1989) 355.
69. S. Bonazzola, E. Gourgoulhon, *Phys. Rev. D* **48** (1993) 2635.
70. N. Stergioulas and J. L. Friedman, *Astrophys. J.* **444** (1995) 306.
71. W. G. Laarakkers, and E. Poisson, *Astrophys. J.* **512** (1999) 282.
72. T. W. Baumgarte, S. L. Shapiro, and M. Shibata, *Astrophys. J.* **528** (2000) L29.
73. M. Ansorg, A. Kleinwächter, and R. Meinel, *Astron. Astrophys.* **381** (2002) L49.
74. R. Birkel, N. Stergioulas, and E. Müller, *Phys. Rev. D* **84** (2011) 023003.
75. J. L. Friedman and N. Stergioulas, *Rotating relativistic stars*, Cambridge University Press, United Kingdom (2013).
76. P. Arumugam, B. K. Sharma, P. K. Sahu, S. K. Patra, T. Sil, M. Centelles and X. Vinas, *Phys. Lett. B* **601** (2004) 51.
77. T. K. Jha, P. K. Raina, P. K. Panda and S. K. Patra, *Phys. Rev. C* **74** (2006) 055803.
78. C. J. Horowitz, J. Pielarewicz, *Phys. Rev. Lett.* **86** (2001) 5647.
79. S. K. Singh, M. Bhuyan, P. K. Panda and S. K. Patra, *J. Phys. G: Nucl. Part. Phys.* **40** (2013) 085104.
80. R. J. Furnstahl, B. D. Serot and H. B. Tang, *Nucl. Phys. A* **598** (1996) 539.
81. H. Müller and B. D. Serot, *Nucl. Phys. A* **606** (1996) 508.
82. R. J. Furnstahl and B. D. Serot, *Nucl. Phys. A* **671** (2000) 447.
83. I. Bednarek and R. Manka, *Int. J. Mod. Phys. D* **10** (2001) 607.
84. I. Bednarek and R. Manka, *Phys. Rev. C* **73** (2006) 045804.
85. B. K. Sharma, P. K. Panda and S. K. Patra, *Phys. Rev. C* **75** (2007) 035808.
86. R. J. Furnstahl, B. D. Serot and H. B. Tang, *Nucl. Phys. A* **615** (1997) 441.
87. S. K. Singh, S. K. Biswal, M. Bhuyan, and S. K. Patra, *Phys. Rev. C* **89** (2014) 044001.
88. S. K. Singh, S. K. Biswal, M. Bhuyan, and S. K. Patra, *J. Phys. G: Part. Nucl. Phys.*

- 41 (2014) 055201.
89. B. D. Serot and J. D. Walecka, in *Advances in Nuclear Physics*, edited by J. W. Negele and Erich Vogt *Plenum Press, New York*, Vol. **16**, p. 1 (1986).
  90. W. Pannert, P. Ring, and J. Boguta, *Phys. Rev. Lett.*, **59** (1986) 2420.
  91. J. Boguta and A. R. Bodmer, *Nucl. Phys. A* **292** (1977) 413.
  92. S. K. Patra, M. Bhuyan, M. S. Mehta and Raj K. Gupta, *Phys. Rev. C* **80** (2009) 034312.
  93. M. Bhuyan, S. K. Patra, and Raj K. Gupta, *Phys. Rev. C* **84** (2011) 014317.
  94. P. -G. Reinhard, *Rep. Prog. Phys.* **52** (1989) 439.
  95. P. Ring, *Prog. Part. Nucl. Phys.* **37** (1996) 193.
  96. J. Meng, H. Toki, S. G. Zhou, S. Q. Zhang, W.-H. Long and L. S. Geng, *Prog. Part. Nucl. Phys.* **57** (2006) 470.
  97. M. Bhuyan, *Phys. Rev. C* **92** (2015) 034323.
  98. H. Liang, J. Meng, and S. G. Zhou, *Phys. Rep.* **570** (2015) 1.
  99. J. Meng and S. G. Zhou, *J. Phys. G: Nucl. Part. Phys.* **42** (2015) 093101.
  100. H. Müller and B. D. Serot, *Nucl. Phys. A* **606** (1996) 508.
  101. B. D. Serot and J. D. Walecka, *Int. J. Mod. Phys. E* **6** (1997) 515.
  102. J. M. Lattimer, and A. W. Steiner, *Eur. Phys. J. A* **50** (2014) 40.
  103. H. Nakada, *Phys. Rev. C* **78** (2008) 054301.
  104. D. Alonso and F. Sammarruca, *Phys. Rev. C* **67** (2003) 054301.
  105. E. N. E. Van Dalen, C. Fuchs and A. Faessler, *Nucl. Phys. A* **744** (2004) 227.
  106. T. Klahn *et al.*, *Phys. Rev. C* **74** (2006) 035802.
  107. P. Danielewicz, R. Lacey and W. G. Lynch, *Science* **298** (2000) 1592.
  108. W. G. Lynch, M. B. Tsang, Y. Zhang, P. Danielewicz, M. Famiano, Z. Li and A. W. Steiner, *Prog. Part. Nucl. Phys.* **62** (2009) 427.
  109. N. K. Glendenning, *Compact Stars, Nuclear Physics, Particle Physics and General Relativity*, New York: Springer (1997).
  110. J. Schaffner-Bielich and A. Gal, *Phys. Rev. C* **62** (1999) 034311.
  111. S. Weissenborn, D. Chatterjee and J. Schaffner-Bielich, *Nucl. Phys. A* **881** (2012) 62.
  112. A. R. Bodmer, *Nucl. Phys. A* **526** (1991) 703.
  113. H. F. Lu, J. Meng, S. Q. Zhang, and S.-G. Zhou, *Euro. Phys. J. A* **17** (2003) 19.
  114. H. F. Lu, X. S. Wang, and Y. Y. Liu, *Comm. Theo. Phys.* **62** (2014) 272.
  115. J. Schaffner, C. B. Dover, A. Gal, D. J. Milliner, C. Greiner and H. Stoecker, *Ann. Phys.* **235** (1994) 35.
  116. J. Boguta and S. Bohrman, *Phys. Lett. B* **102** (1981) 93.
  117. N. K. Glendenning, S. A. Moszkowski, *Phys. Rev. Lett.* **67** (1991) 2414.
  118. M. Chiapparini, M. E. Bracco, A. Delfino, M. Malheiro, D. P. Menezes and C. Providencia, *Nucl. Phys. A* **826** (2009) 178.
  119. A. W. Steiner, S. Reddy and M. Prakash, *Phys. Rev. D* **66** (2002) 094007.
  120. A. W. Steiner, J. M. Lattimer and E. F. Brown, *Astrophys. J.* **722** (2010) 33.
  121. B. S. Sathyaprakash and B. F. Schutz, *Liv. Rev. Rel.* **12** (2009) 2.
  122. S. van Straaten, E. C. Ford, M. van der Klis, M. Méndez and P. Kaaret *Astrophys. J.* **540** (2000) 1049.
  123. F. Sammarruca, *Phys. Rev. C* **79** (2009) 034301.
  124. M. Dutra *et al.*, *Phys. Rev. C* **85** (2012) 035201.
  125. Roy P. Kerr, *Phys. Rev. Lett* **11** (1963) 237.